



Improved Explicit Integration Algorithms with Controllable Numerical Damping for Real-Time Hybrid Simulation

Wei Guo¹; Yanxia Zhu²; Xiaoli Wu³; and Yujie Yu⁴

Abstract: The paper proposes an improved single-step method of explicit displacement and velocity (SSMEDV) with controllable numerical damping based on the discrete control theory, which can be applied to real-time hybrid simulation (RTHS). The stability, overshoot, and numerical damping characteristics of the proposed algorithms are studied. It is shown that certain algorithms have unconditional stability for linear and softening nonlinear structures. The overshoot phenomenon is small, where the displacement is one power of the time step due to the initial velocity, whereas the velocity does not. The amount of numerical damping is adjusted by a single parameter to control the divergence of false higher-order modes. The analysis of RTHS was performed on a multiple degrees-of-freedom (MDOF) structure and complex building-damper structure to verify the theoretical analysis. The comparison with two typical algorithms of the explicit Newmark and Gui- λ demonstrates the effectiveness of the proposed algorithms in improving stability, accuracy, and computational efficiency, which can be applied to complex RTHS. DOI: [10.1061/\(ASCE\)EM.1943-7889.0002163](https://doi.org/10.1061/(ASCE)EM.1943-7889.0002163). © 2023 American Society of Civil Engineers.

Author keywords: Real-time hybrid simulation (RTHS); Single-step method of explicit displacement and velocity (SSMEDV); Nonlinear structure; Numerical damping; Computational efficiency.

Introduction

With the development of the economy and the advancement of science and technology, many infrastructures, such as large bridges and high-rise and large-span buildings, have been built (Yu et al. 2019). Traditional test methods have their limitations; for example, the static test only considers static effects (Jiang et al. 2012), the pseudodynamic test cannot test velocity-dependent components (Guo et al. 2019), and the shaking table test has size effects (Wang and Zhang 2017). Real-time hybrid simulation (RTHS) (Nakashima et al. 1992; Li et al. 2017) is an advanced testing technology to assess dynamic responses of structures. It has low demand for experimental fields and equipment, and can accomplish a full-scale test, which is more economical and accurate than traditional tests. The RTHS divides the structure under investigation into numerical and physical substructures, where the former is analytically modeled by finite-element software and the latter is physically tested in the laboratory (Zhu et al. 2019; Gu et al. 2021; Huang et al. 2022). Thus, RTHS combines the advantages of numerical simulation and experimental test.

Integration algorithms are used in the numerical substructure to generate command displacement for the physical substructure. However, there are inevitably a series of challenges for integration algorithms in RTHS (Peng 2016). The integration algorithms should have sufficient stability and accuracy to assure the testing progress smoothly and accurately (Wu et al. 2005, 2006, 2009), and have good computational efficiency to meet the requirement of real-time interaction between the physical and numerical substructures.

Integration algorithms are generally classified as explicit and implicit according to whether or not state quantities in the current step can be expressed by state quantities of the previous steps. Explicit integration algorithms have high computational efficiency because of no iterations, but most of them are conditionally stable because the stability is restricted by large time steps (Rezaiee-Pajand et al. 2021), which leads to longer computing time and larger data. Unconditional stability is the advantage of most implicit integration algorithms, but their low computational efficiency is very unfavorable to the real-time requirement of RTHS. Therefore, an integration algorithm with explicit calculation and unconditional stability is more suitable for RTHS, which has attracted great attention.

Chen and Ricles (2008, 2010) utilized a pole mapping method to develop an unconditionally stable CR algorithm in which the displacement and velocity calculations are explicit. Gui et al. (2014) proposed a family of explicit algorithms with a controlled parameter λ , and certain subfamilies were found to be unconditionally stable for any system state (linear elastic, stiffness softening, or stiffness hardening). But their proposed algorithms had no numerical damping, so they cannot suppress the divergence problem of false higher-order modes (Kolay and Ricles 2019; Yang et al. 2020; Tang et al. 2021). Newmark (1959) proposed the Newmark family of algorithms with two controlled parameters: γ and β . When $\gamma > 0.5$, the algorithms are implicit and unconditionally stable, and the appropriate numerical damping can be obtained by adjusting the parameter γ . Many algorithms have been improved based on the Newmark family of algorithms, such as the KR algorithm (Kolay and Ricles 2014), Gui- λ algorithms (Gui et al. 2014), and generalized CR algorithms (Fu et al. 2019).

¹Professor, National Engineering Research Center of High-Speed Railway Construction Technology, School of Civil Engineering, Central South Univ., Changsha, Hunan 410075, China. Email: guowei@csu.edu.cn

²National Engineering Research Center of High-Speed Railway Construction Technology, School of Civil Engineering, Central South Univ., Changsha, Hunan 410075, China. Email: 2919387935@qq.com

³Dongxihu District Municipal Urban-Rural Development Bureau, 53 Wuhuan Ave., Wujiashan St., Dongxihu District, Wuhan, Hubei 430040, China. Email: 2942711964@qq.com

⁴Professor, National Engineering Research Center of High-Speed Railway Construction Technology, School of Civil Engineering, Central South Univ., Changsha, Hunan 410075, China (corresponding author). ORCID: <https://orcid.org/0000-0002-1732-4023>. Email: yujiecsu@csu.edu.cn

Note. This manuscript was submitted on December 9, 2021; approved on July 16, 2022; published online on January 17, 2023. Discussion period open until June 17, 2023; separate discussions must be submitted for individual papers. This paper is part of the *Journal of Engineering Mechanics*, © ASCE, ISSN 0733-9399.

Many algorithms have been proposed and studied; however, due to the coupling of physical substructure and numerical substructure in RTHS, the integration algorithms present completely different numerical properties (Wu et al. 2005, 2006, 2009). Wu et al. (2005) applied the central difference method (CDM) algorithm to RTHS, and the results demonstrated that the stability and accuracy of the integration algorithm were reduced in RTHS. The stability of the CDM algorithm decreased with the increase of the mass of physical substructure (Wu et al. 2009). Zhu et al. (2015) used discrete control theory to analyze the stability of KR algorithm (Kolay and Ricles 2014) in multiple degrees-of-freedom (MDOF) RTHS and compared the effects of seven classical integration algorithms on the delay-dependent stability and accuracy of MDOF RTHS (Zhu et al. 2016). Li et al. (2021) established a discrete stability analysis method for integration algorithms applied to RTHS and studied the influence of the substructures partition method, damping ratio, and time-step size on stability.

In this paper, a new family of explicit integration algorithms with adjustable numerical damping is proposed by improving Gui- λ algorithms based on the Newmark family of algorithms. The proposed algorithms are more generalized and have more versatile numerical properties than the explicit Newmark algorithm and Gui- λ algorithms. The numerical characteristics of the proposed algorithms and their application in RTHS are studied thoroughly. The paper is organized as follows: firstly, improved explicit integration algorithms are proposed by the transfer function method. Secondly, the numerical properties of the algorithms are studied by theoretical analysis and numerical work. Moreover, the algorithms are verified by two types of MDOF real-time simulations. Finally gives the conclusions.

Improved Explicit Integration Algorithms

Integration algorithms are widely used to solve structural dynamics equations, and for a linear MDOF structural system, the equations can be expressed

$$\mathbf{M}\ddot{\mathbf{X}}_{i+1} + \mathbf{C}\dot{\mathbf{X}}_{i+1} + \mathbf{K}\mathbf{X}_{i+1} = \mathbf{F}_{i+1} \quad (1)$$

where \mathbf{M} , \mathbf{C} , and \mathbf{K} are the mass, damping, and stiffness matrices respectively; $\ddot{\mathbf{X}}_{i+1}$, $\dot{\mathbf{X}}_{i+1}$, and \mathbf{X}_{i+1} are the acceleration, velocity, and displacement vectors at the $(i+1)$ th time step, respectively; and \mathbf{F}_{i+1} is the external force vector. The general single-step integration algorithm, where the velocity vector $\dot{\mathbf{X}}_{i+1}$ and displacement vector \mathbf{X}_{i+1} are dependent on structural responses (acceleration, velocity, and displacement) at the i th or the $(i+1)$ th time step, is assumed as follows:

$$\begin{aligned} \mathbf{X}_{i+1} &= \mathbf{a}_1\mathbf{X}_i + \mathbf{a}_2\dot{\mathbf{X}}_i\Delta t + \mathbf{a}_3\ddot{\mathbf{X}}_i\Delta t^2 + \mathbf{a}_4\dot{\mathbf{X}}_{i+1}\Delta t + \mathbf{a}_5\ddot{\mathbf{X}}_{i+1}\Delta t^2 \\ \dot{\mathbf{X}}_{i+1} &= \mathbf{b}_1\dot{\mathbf{X}}_i + \mathbf{b}_2\ddot{\mathbf{X}}_i\Delta t + \mathbf{b}_3\ddot{\mathbf{X}}_{i+1}\Delta t \end{aligned} \quad (2)$$

where Δt = time-step size; and \mathbf{a}_i and \mathbf{b}_i are two matrices of corresponding integration coefficients, which determine the numerical properties of algorithms. Eq. (1) can be integrated with Eq. (2) when \mathbf{a}_i and \mathbf{b}_i are known.

The Newmark family of algorithms is a kind of time-step method proposed by Newmark (1959). The algorithms use two parameters, γ and β , to determine the numerical characteristics.

When $\gamma > 0.5$, the algorithms are implicit and unconditionally stable, and the appropriate numerical damping can be obtained by adjusting the parameter γ . The algorithms are as follows:

$$\begin{aligned} \mathbf{X}_{i+1} &= \mathbf{X}_i + \dot{\mathbf{X}}_i\Delta t + (0.5 - \beta)\ddot{\mathbf{X}}_i\Delta t^2 + \beta\ddot{\mathbf{X}}_{i+1}\Delta t \\ \dot{\mathbf{X}}_{i+1} &= \dot{\mathbf{X}}_i + (1 - \gamma)\ddot{\mathbf{X}}_i\Delta t + \gamma\ddot{\mathbf{X}}_{i+1}\Delta t \end{aligned} \quad (3)$$

When $\gamma = 0.5$ and $\beta = 0$, the algorithm is called the explicit Newmark algorithm, but only the expression of displacement is an explicit form. Correspondingly, Eq. (3) is rewritten as follows:

$$\begin{aligned} \mathbf{X}_{i+1} &= \mathbf{X}_i + \dot{\mathbf{X}}_i\Delta t + 0.5\ddot{\mathbf{X}}_i\Delta t^2 \\ \dot{\mathbf{X}}_{i+1} &= \dot{\mathbf{X}}_i + 0.5\ddot{\mathbf{X}}_i\Delta t + 0.5\ddot{\mathbf{X}}_{i+1}\Delta t \end{aligned} \quad (4)$$

Gui- λ algorithms are a family of integration algorithms with explicit displacement and velocity (Gui et al. 2014). They were developed by assigning the eigenvalues of the Newmark family at $\gamma = 0.5$ to the poles of their discrete transfer function, which results in no adjustable numerical damping

$$\begin{aligned} \mathbf{X}_{i+1} &= \mathbf{X}_i + \dot{\mathbf{X}}_i\Delta t + \alpha\ddot{\mathbf{X}}_i\Delta t^2 \\ \dot{\mathbf{X}}_{i+1} &= \dot{\mathbf{X}}_i + \alpha\ddot{\mathbf{X}}_{i+1}\Delta t \\ \alpha &= 2\lambda[2\lambda\mathbf{M} + \lambda\Delta t\mathbf{C} + 2\Delta t^2\mathbf{K}]^{-1}\mathbf{M} \end{aligned} \quad (5)$$

where the subfamily with λ is derived from the Newmark family with $\gamma = 0.5$ and $\beta = 1/\lambda$. Obviously, the subfamily with $\lambda = \infty$ is exactly similar to the explicit Newmark algorithm.

To improve Gui- λ algorithms based on the Newmark family of algorithms, a new family of explicit and unconditionally stable integration algorithms with adjustable numerical damping is proposed by involving all γ values from the Newmark family of algorithms. The proposed algorithms are defined as follows:

$$\begin{aligned} \mathbf{X}_{i+1} &= \mathbf{X}_i + \dot{\mathbf{X}}_i\Delta t + \alpha_1\ddot{\mathbf{X}}_i\Delta t^2 \\ \dot{\mathbf{X}}_{i+1} &= \dot{\mathbf{X}}_i + \alpha_2\ddot{\mathbf{X}}_i\Delta t \end{aligned} \quad (6)$$

where α_1 and α_2 = parameters of proposed algorithms. Because the proposed algorithms are a single-step method of explicit displacement and velocity, they can be named the single-step method of explicit displacement and velocity (SSMEDV) algorithms.

Next, the parameters α_1 and α_2 are given. The performance of algorithms can be characterized by the eigenvalues of the transfer function. The parameters α_1 and α_2 were derived by using the eigenvalues of SSMEDV algorithms equal to those of the Newmark family of algorithms. Firstly, the z transforms of Eqs. (1) and (6) can be expressed

$$\mathbf{M}\ddot{\mathbf{X}}_{i+1}(z) + \mathbf{C}\dot{\mathbf{X}}_{i+1}(z) + \mathbf{K}\mathbf{X}_{i+1}(z) = \mathbf{F}_{i+1}(z) \quad (7)$$

$$\begin{aligned} \dot{\mathbf{X}}_{i+1}(z) &= \frac{(z-1)\alpha_2}{(z-1)\alpha_1 + \alpha_2}\mathbf{X}_{i+1}(z)/\Delta t \\ \ddot{\mathbf{X}}_{i+1}(z) &= \frac{(z-1)^2}{(z-1)\alpha_1 + \alpha_2}\mathbf{X}_{i+1}(z)/\Delta t^2 \end{aligned} \quad (8)$$

where $\ddot{\mathbf{X}}_{i+1}(z)$, $\dot{\mathbf{X}}_{i+1}(z)$, $\mathbf{X}_{i+1}(z)$, and $\mathbf{F}_{i+1}(z) = z$ transforms of $\ddot{\mathbf{X}}_{i+1}$, $\dot{\mathbf{X}}_{i+1}$, \mathbf{X}_{i+1} , and \mathbf{F}_{i+1} , respectively. Substituting Eq. (8) into Eq. (7) leads to the corresponding transfer function as follows:

$$G(z) = \frac{\mathbf{X}_{i+1}(z)}{\mathbf{F}_{i+1}(z)} = \frac{\alpha_1\Delta t^2 z + (\alpha_2 - \alpha_1)\Delta t^2}{\mathbf{M}z^2 + (\alpha_1\mathbf{K}\Delta t^2 + \alpha_2\mathbf{C}\Delta t - 2\mathbf{M})z + \mathbf{M} + (\alpha_2 - \alpha_1)\mathbf{K}\Delta t^2 - \alpha_2\mathbf{C}\Delta t} \quad (9)$$

Table 1. Coefficient matrices of discrete transfer function for SSMEDV algorithms

N-subscript	N-value	D-subscript	D-value
N_2	0	D_2	\mathbf{M}
N_1	$\alpha_1 \Delta t^2$	D_1	$\alpha_1 \mathbf{K} \Delta t^2 + \alpha_2 \mathbf{C} \Delta t - 2\mathbf{M}$
N_0	$(\alpha_2 - \alpha_1) \Delta t^2$	D_0	$\mathbf{M} + (\alpha_2 - \alpha_1) \mathbf{K} \Delta t^2 - \alpha_2 \mathbf{C} \Delta t$

The coefficient matrices values of $G(z)$ divided into the numerator and denominator, indicated as N/D-subscript and N/D-value, are listed in Table 1.

The subscripts N and D represent the order of z . Similarly, the Newmark family of algorithms is z transformed, and the coefficient matrices values of the numerator and denominator of $G(z)$ are listed in Table 2.

Lastly, the parameters α_1 and α_2 can be obtained by the denominator coefficient matrices of SSMEDV algorithms proportional to those of Newmark family of algorithms. When the structure is nonlinear, the parameters α_1 and α_2 are assumed to be invariant to improve the computational efficiency, and are determined from the initial damping matrix \mathbf{C}_0 and stiffness matrix \mathbf{K}_0 , which are as follows:

$$\begin{aligned}\alpha_1 &= \frac{(1+2\gamma)\mathbf{M}}{2\beta\mathbf{K}_0\Delta t^2 + 2\gamma\mathbf{C}_0\Delta t + 2\mathbf{M}}, \\ \alpha_2 &= \frac{\mathbf{M}}{\beta\mathbf{K}_0\Delta t^2 + \gamma\mathbf{C}_0\Delta t + \mathbf{M}}\end{aligned}\quad (10)$$

The subfamilies with $\gamma = 0.5$ are the same as the Gui- λ algorithms, which shows that the proposed algorithms contain the well-known Gui- λ algorithms as a special case.

Numerical Properties

Improved explicit integration algorithms have been proposed in the preceding section. Here, their numerical properties are discussed. Because the characteristics of the MDOF structure remain unchanged after modal decoupling, the single degree of freedom (SDOF) structure was used to analyze the numerical properties of algorithms, and its diagram is shown schematically in Fig. 1.

Stability

The stability of algorithms reflects the anti-interference ability of system to external excitation. According to discrete control theory, the stability of algorithms is usually judged by whether the maximum eigenvalue of transfer function is less than 1, and the influence of parameter variation on system stability is analyzed by the root locus method (Franklin et al. 2002). Therefore, the stable condition of SSMEDV algorithms was determined by the discrete control theory in this section. Linear and nonlinear systems are considered.

Linear-Elastic System

For a linear-elastic system, $G(z)$ is presented in Eq. (9), and its characteristic equation can be obtained by making the denominator zero. The characteristic equation of SSMEDV algorithms under

SDOF can be revised as follows:

$$A_1 z^2 + A_2 z + A_3 = 0 \quad (11)$$

where A_1 , A_2 , and A_3 = coefficient of denominator of $G(z)$, where $A_1 = 1$, $A_2 = \alpha_1 \Omega^2 + 2\alpha_2 \xi \Omega - 2$, $A_3 = (\alpha_2 - \alpha_1) \Omega^2 - 2\alpha_2 \xi \Omega + 1$, $\Omega = \omega \Delta t$, $\omega^2 = k/m$, and $\xi = c/(2\omega m)$.

According to Eq. (11), the eigenvalues of $G(z)$ can be expressed

$$z_{1,2} = \frac{-A_2 \pm \sqrt{A_2^2 - 4A_1A_3}}{2A_1} \quad (12)$$

Only when the two principal eigenvalues are conjugate complex numbers can the structural dynamic equations be expressed in the form of vibration, so the following conditions must be met:

$$A_2^2 - 4A_1A_3 < 0 \quad (13)$$

$$|z_{1,2}| = \frac{\sqrt{(-A_2)^2 + (\sqrt{-A_2^2 + 4A_1A_3})^2}}{2A_1} = \sqrt{\frac{A_3}{A_1}} \leq 1 \quad (14)$$

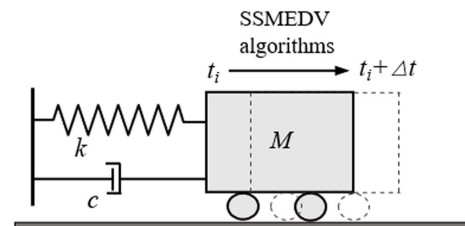
Substituting Eq. (11) into Eqs. (13) and (14) leads to the following stability condition of SSMEDV algorithms for the linear-elastic system:

$$\begin{aligned}\alpha_1^2 \Omega^2 + 4\alpha_1 \alpha_2 \xi \Omega + 4\alpha_2^2 \xi^2 - 4\alpha_2 &< 0 \\ (\alpha_2 - \alpha_1) \Omega^2 - 2\alpha_2 \xi \Omega &\leq 0\end{aligned}\quad (15)$$

Lastly, Eq. (10) is substituted into Eq. (15) for simplification, which indicates that the algorithms are unconditionally stable when $\gamma \geq 1/2$ and $\beta \geq (2\gamma + 1)^2/16$. The stability property of SSMEDV algorithms for several γ and β values is plotted in Fig. 2. It can be seen from Fig. 2(a) that the root trajectories of algorithms satisfying the aforementioned stability condition are all in the stable circle. In addition, in Fig. 2(b), the stability of algorithms increased as γ increased, whereas it decreased as β increased.

System with Nonlinear Stiffness

In tests, the structures sometimes enter a nonlinear stage under strong external excitation (Yang et al. 2017), which reduces the stability of integration algorithms to some extent (Chen and Ricles 2008; Chang 2014; Feng et al. 2018). Therefore, it is necessary

**Fig. 1.** SDOF system.**Table 2.** Coefficient matrices of discrete transfer function for Newmark family of algorithms

N-subscript	N-value	D-subscript	D-value
N_2	$2\beta \Delta t^2$	D_2	$2\beta \mathbf{K} \Delta t^2 + 2\gamma \mathbf{C} \Delta t + 2\mathbf{M}$
N_1	$(2\gamma - 4\beta + 1) \Delta t^2$	D_1	$(2\gamma - 4\beta + 1) \mathbf{K} \Delta t^2 + \mathbf{C} \Delta t (2 - 4\gamma) - 4\mathbf{M}$
N_0	$(2\beta - 2\gamma + 1) \Delta t^2$	D_0	$(2\beta - 2\gamma + 1) \mathbf{K} \Delta t^2 + \mathbf{C} \Delta t (2\gamma - 2) + 2\mathbf{M}$

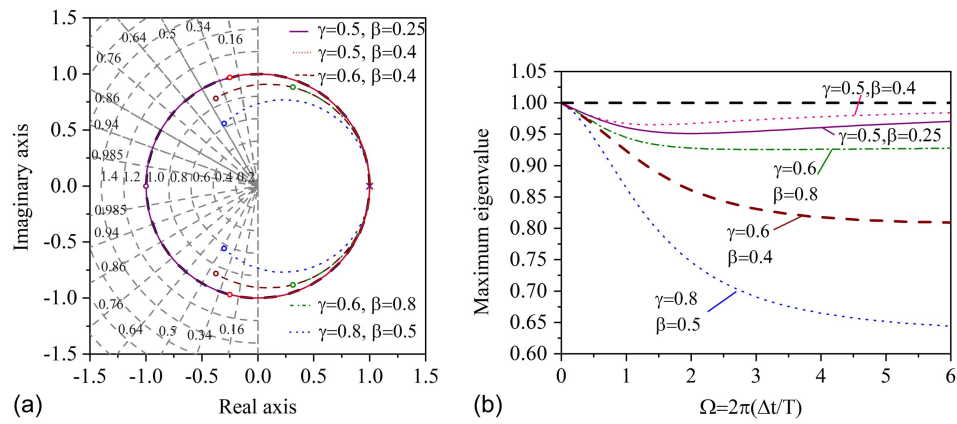


Fig. 2. Stability property of SSMEDV algorithms in numerical analysis: (a) root locus diagram; and (b) maximum eigenvalue diagram.

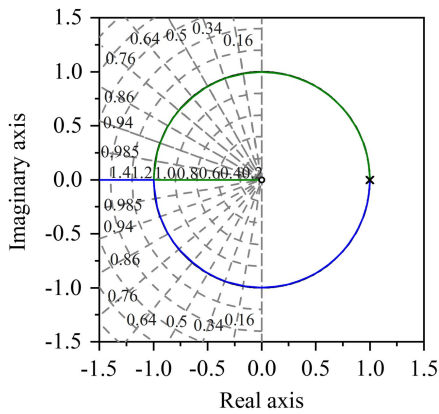


Fig. 3. Root locus for system with nonlinear stiffness.

to analyze the performance of the integration algorithms for nonlinear structures. Structural nonlinearity can be divided into softening and hardening (Liang and Mosalam 2016). For a small time-step size, the stiffness can be regarded as a certain value, so the nonlinear SDOF structural motion equation can be approximated in an incremental form as follows:

$$m\Delta\ddot{x}_i + c\Delta\dot{x}_i + k_i\Delta x_i = \Delta F_i \quad (16)$$

where k_i = tangent stiffness for the i th time step; $\Delta\ddot{x}_i$, $\Delta\dot{x}_i$, Δx_i , and ΔF_i = increments of acceleration, velocity, displacement, and

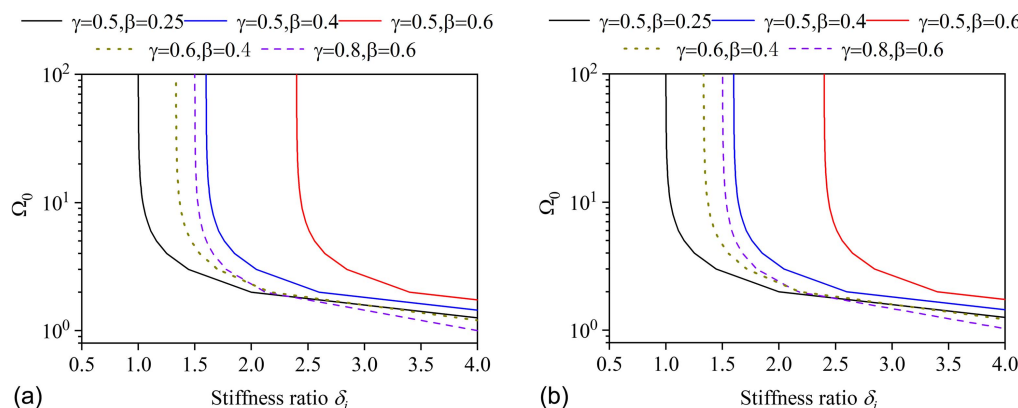


Fig. 4. Relationship between the stiffness ratio and Ω_0 : (a) $\xi = 0$; and (b) $\xi = 0.05$.

external force, defined as $\Delta\ddot{x}_i = \ddot{x}_{i+1} - \ddot{x}_i$, $\Delta\dot{x}_i = \Delta\dot{x}_{i+1} - \Delta\dot{x}_i$, $\Delta x_i = \Delta x_{i+1} - \Delta x_i$, and $\Delta F_i = \Delta F_{i+1} - \Delta F_i$.

Eq. (16) corresponds to a closed-loop system, in which the tangent stiffness k_i is used as the feedback factor. SSMEDV algorithms are substituted into Eq. (16) to obtain the characteristic equation of the closed-loop system

$$1 + k_i \frac{(z-1)\alpha_1 + \alpha_2}{(z-1)(m \cdot (z-1)/\Delta t^2 + c \cdot \alpha_2/\Delta t)} = 0 \quad (17)$$

The root locus for the case of $m = 80$ kg, $\Omega = 0.01\pi$, $\xi = 0.05$, $\Delta t = 0.01$, and $k_0 = 789.6$ N/m is shown in Fig. 3. One branch of the locus crosses the unit circle at $z = -1$, which means that SSMEDV algorithms are stable only for a finite range of k_i . By substituting $z = -1$ into Eq. (17), the stability condition can be obtained as follows:

$$\delta_i = \frac{k_i}{k_0} \leq \frac{2\beta}{\gamma} + \frac{2}{\gamma\Omega_0^2} + \frac{2(2\gamma-1)\xi}{\gamma\Omega_0} \quad (18)$$

Eq. (18) is visually drawn in Fig. 4. It is shown that the stiffness ratio of SSMEDV algorithms exceeded the value of 1 when the Ω_0 is arbitrary, which indicates that the algorithms are unconditionally stable for both linear and softening nonlinear structures, but they must satisfy the premise of $\gamma \geq 1/2$ and $\beta \geq (2\gamma+1)^2/16$. With the increases of stiffness ratio, Ω_0 continuously decreased and eventually flattened, which reveals that the algorithms applied to structures with large hardening nonlinearity can be stabilized by reducing the time steps appropriately.

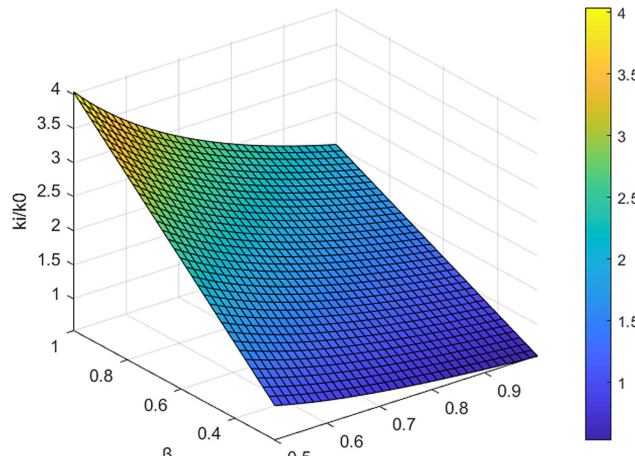


Fig. 5. Influence of parameters on the stiffness ratio.

Fig. 5 illustrates the relation between the two parameters and the stiffness ratio. It is observed that the stiffness ratio increased as β increased, but decreased as γ increased. According to the nonlinear optimal solution of fmincon in MATLAB version R2020a, when $[\gamma, \beta] = [0.5, 1]$, the maximum stiffness ratio was 4.04 to achieve the unconditional stability of algorithms for hardening nonlinear structures.

Accuracy

Because the SSMEDV algorithms and Newmark family of algorithms have the same eigenvalues, the two algorithms have similar accuracy. The SSMDV algorithms have second-order accuracy when $\gamma = 1/2$, and they have first-order accuracy when $\gamma \neq 1/2$. To better illustrate how the value of γ and β affect the accuracy, it can be characterized by numerical damping $\bar{\xi}$ and periodic decay rate (PE) (Chopra 2001). In the case that the eigenvalues of the algorithms are a pair of conjugate complex numbers, the numerical damping and periodic decay rate are calculated by

$$z_{1,2} = \frac{-A_2 \pm i\sqrt{4A_1A_3 - A_2^2}}{2A_1} = A + Bi; \quad \bar{\Omega} = \arctan(B/A) \quad (19)$$

$$\bar{\xi} = -\ln(A^2 + B^2)/2\bar{\Omega}; \quad PE = (\bar{T} - T)/T = (\Omega - \bar{\Omega})/\bar{\Omega} \quad (20)$$

Fig. 6 shows the numerical damping and periodic decay rate for SSMEDV algorithms. As shown in Fig. 6(a), when $\gamma = 1/2$, the

algorithms had no numerical damping, but when $\gamma > 1/2$, the algorithms introduced positive numerical damping, which makes structural vibration attenuated even when there is no real damping, and the numerical damping increased as γ increased. Fig. 6(b) indicates the periodic decay rate increased as β increased for a given γ . As a result, $\gamma \geq 1/2$ and $\beta = (2\gamma + 1)^2/16$ are the best accuracy for the algorithms.

Overshoot

Goudreau and Taylor (1973) found that the overshoot phenomenon is an important performance of algorithms, and it far exceeds the exact solution in the initial few steps. The overshoot can be determined by a higher power of Ω between the displacement and velocity of a SDOF structure with free vibration and the corresponding initial value at $\Omega \rightarrow \infty$. To analyze the overshoot of SSMEDV algorithms, firstly, the SDOF structural dynamic equation as Eq. (21) is substituted into Eq. (6), which can be obtained by Eq. (22)

$$m\ddot{x}_i + k_i x_i = 0 \quad (21)$$

$$\begin{aligned} x_{i+1} &= \left(1 - \alpha_1 \frac{k_i}{m} \Delta t^2\right) x_i + \dot{x}_i \Delta t \\ \dot{x}_{i+1} &= -\alpha_2 \frac{k_i}{m} \Delta t x_i + \dot{x}_i \end{aligned} \quad (22)$$

Secondly, Eq. (10) is revised into the formula under the SDOF structure, which is substituted into Eq. (22), and when Ω ($\Omega = \omega \Delta t$) $\rightarrow \infty$, Eq. (22) can be simplified by

$$\begin{aligned} x_{i+1} &\approx \left(1 - \frac{1+2\gamma}{2\beta} \cdot \frac{k_i}{k_0}\right) x_i + \dot{x}_i \Delta t \\ \dot{x}_{i+1} &\approx -\frac{1}{\beta \Delta t} \cdot \frac{k_i}{k_0} x_i + \dot{x}_i \end{aligned} \quad (23)$$

According to Eq. (23), the structural nonlinearity does not affect the overshoot effect. In addition, the displacement and time step have one power overshoot effect due to the initial velocity, but the velocity does not.

Lastly, the SDOF structure in Fig. 1 was used as a numerical example to verify the overshoot effect of the algorithms. In this example, the time step ($dt/T_0 = 10$) is sufficient and the initial conditions are $x_0 = 1$ mm and $v_0 = 0$. The SSMEDV algorithms with parameters $[\gamma, \beta] = [0.5, 0.25]$ and $[\gamma, \beta] = [0.6, 0.4]$ were adopted to linear and nonlinear structures, as shown in Figs. 7 and 8.

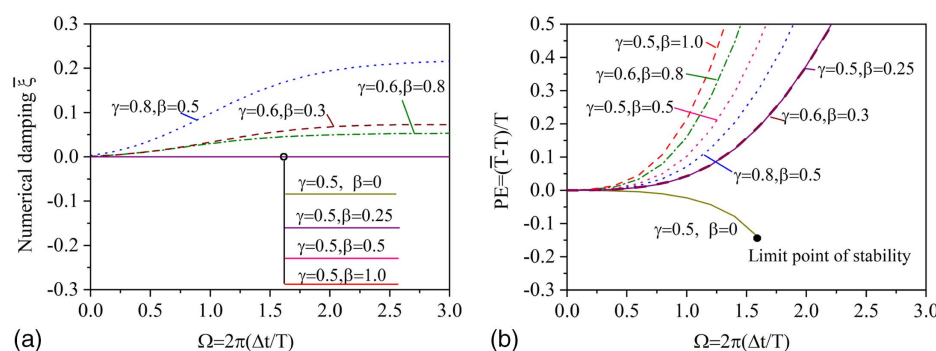


Fig. 6. Accuracy property of SSMEDV algorithms: (a) numerical damping; and (b) periodic decay rate.

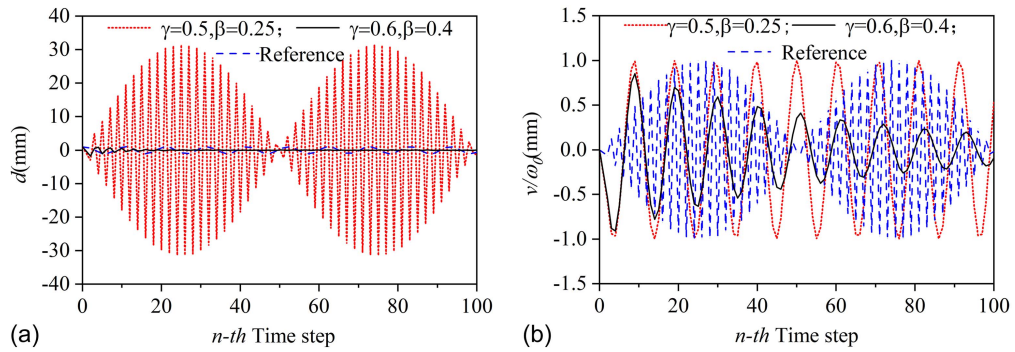


Fig. 7. Overshoot response for linear structure: (a) displacement; and (b) velocity.

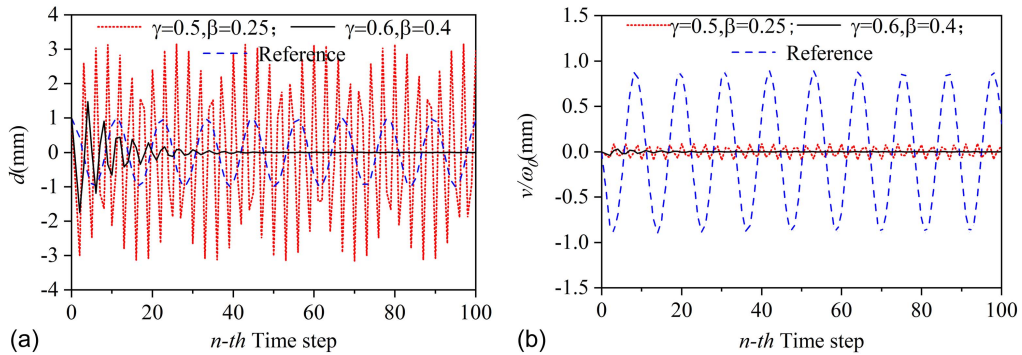


Fig. 8. Overshoot response for nonlinear structure ($d_i/T_0 = 10$ and $k_i = 0.8 \times k_0$): (a) displacement; and (b) velocity.

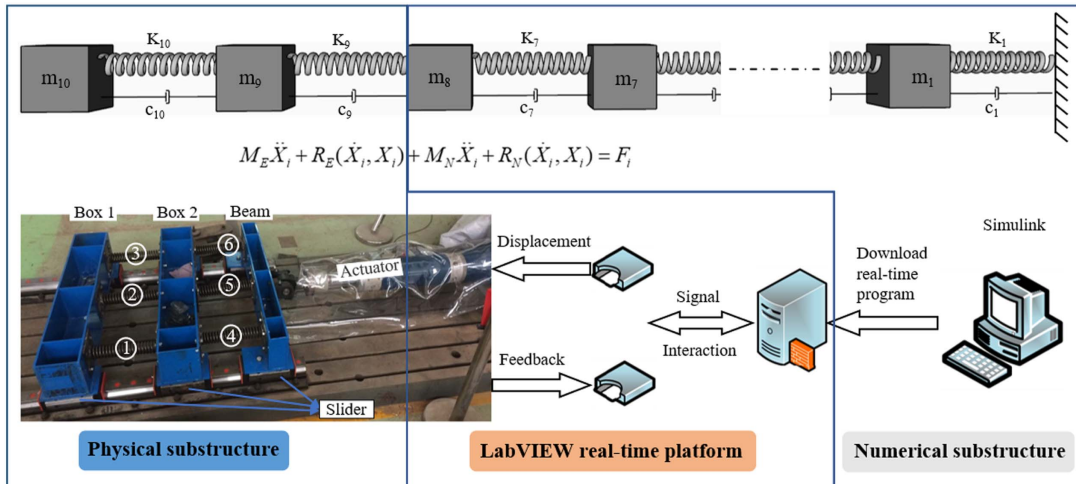


Fig. 9. Description of RTHS for MDOF structure. (Image by authors.)

The results demonstrate that the displacement had a large overshoot effect, but the velocity did not. Besides, it is obvious that the overshoot effect under $[\gamma, \beta] = [0.6, 0.4]$ was smaller than that under $[\gamma, \beta] = [0.5, 0.25]$, which indicates the advantage of SSMEDV algorithms in adjustable numerical damping.

Numerical Simulation

MDOF Structure

The MDOF structure was a spring-mass-damping system with 10 degrees of freedom (DOFs). Box 1 with Springs 1 and 3 and

Box 2 with Springs 4 and 6 from the spring mass box models were selected as the physical substructure, as shown in Fig. 9.

The test setup consisted of three parts: physical substructure, numerical substructure, and LabVIEW version 19.0.1(32-bit) real-time platform. Firstly, the numerical model established in a finite-element software was downloaded to the LabVIEW real-time platform. Secondly the displacement response calculated by integration algorithms was loaded on the physical substructure in real time. Finally, the feedback force of physical substructure was transmitted to the LabVIEW real-time platform to participate in the calculation of numerical model. This process was repeated until the end of whole test.

Table 3. Numerical and physical substructure parameters

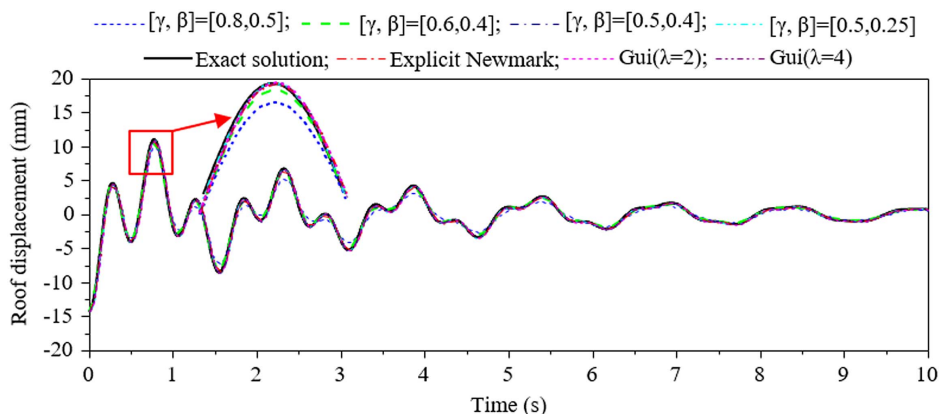
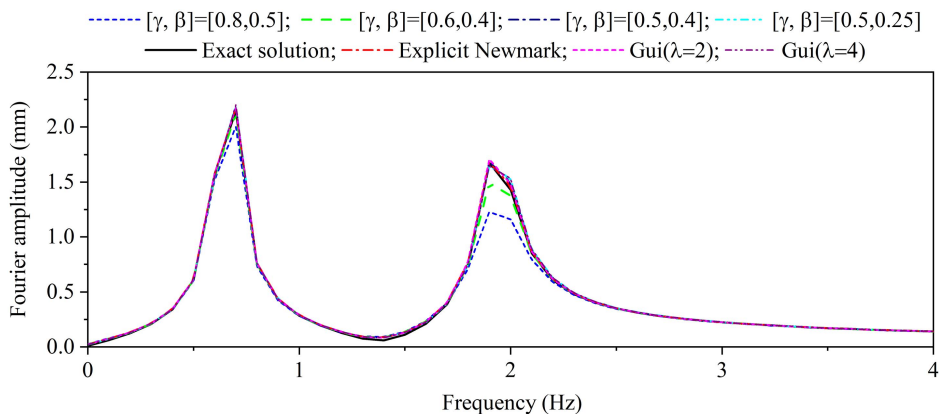
Structure	Mass (kg)	Stiffness (N/mm)	Damping (ratio)
Numerical substructure (8-DOF)	155.6	100	5%
Physical substructure (2-DOF)	81.2; 81.6	77.7; 74.8	27.5

The Servertest single-shaft system in the National Engineering Research Center of High-Speed Railway Construction Technology, Central South University, was adopted as the loading actuator model, in which the third-order polynomial method (Guo et al. 2016; Enokida et al. 2015) was used to compensate the delay of actuator. To ensure the synchronization of physical and numerical substructures, the displacement response was processed by linear interpolation algorithm (Chen et al. 2009) to obtain the same frequency as the physical substructure. The material performance was tested prior to simulation, which was given in Table 3. The first three and the highest structural vibration frequencies were 0.6, 1.9, 3.0, and 8.3 Hz, respectively, and the mass ratio was 0.11. In this section, the SSMEDV algorithms were compared with two typical algorithms of the explicit Newmark and Gui- λ in the numerical damping, time steps, and computational efficiency.

Firstly, in the numerical damping, two working conditions based on different modal combinations, namely Case 1 with $x_0 = \Phi_1 + 0.5 \times \Phi_2$ and $v_0 = 0$, and Case 2 with $x_0 = \Phi_1 + 0.5 \times \Phi_2 + 0.5 \times \Phi_8$ and $v_0 = 0$, were designed for simulation analysis.

The sampling frequency is 1,024 Hz, and the time step is 10/1,024 s. In Case 1, the structure vibrated mainly in the first mode. Fig. 10 presents that the solution of algorithms is similar to the exact solution except for the two SSMEDV algorithms with parameters $[\gamma, \beta] = [0.8, 0.5]$ and $[\gamma, \beta] = [0.6, 0.4]$. This is because the structural response of two algorithms at the second-order frequency is weakened by the numerical damping, as shown in Fig. 11. In Case 2, results were the same for selecting one of the sixth through 10th modes, so the representative eighth mode is added to display, which is to simulate the high-frequency response from the inevitable systematic error of physical equipment in tests. Figs. 12 and 13 show that the additional high-frequency response is weakened by the strong numerical damping under $[\gamma, \beta] = [0.8, 0.5]$, so the response of the algorithm was closer to the exact response than that of other algorithms. In summary, the numerical damping of SSMEDV algorithms can be adjusted to obtain better accuracy.

Secondly, the algorithms applied to RTHS are conditionally stable and thus have time-step constraints. Improving the mass ratio was more conducive to analyzing the influence of time step on the stability of algorithms (Wu et al. 2009). Thus, the weight of 80 kg was added to each mass box, and the mass ratio was adjusted to 0.42. The maximum structural vibration frequency was 83.4 Hz. When the time step was increased to 25/1,024 s, Fig. 14 displays that only Gui($\lambda = 2$) algorithm and SSMEDV algorithms with parameters $[\gamma, \beta] = [0.6, 0.4]$ and $[\gamma, \beta] = [0.8, 0.5]$ were stable,

**Fig. 10.** Time-domain displacement response of structure in Case 1.**Fig. 11.** Frequency-domain displacement response of structure in Case 1.

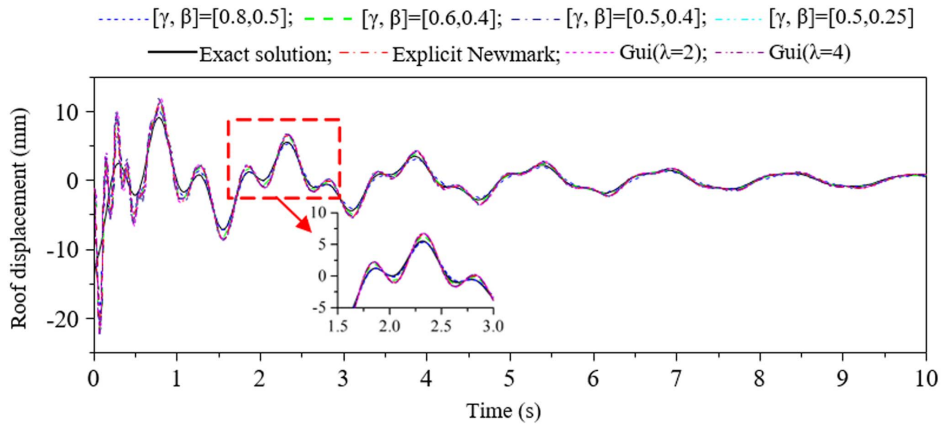


Fig. 12. Time-domain displacement response of structure in Case 2.

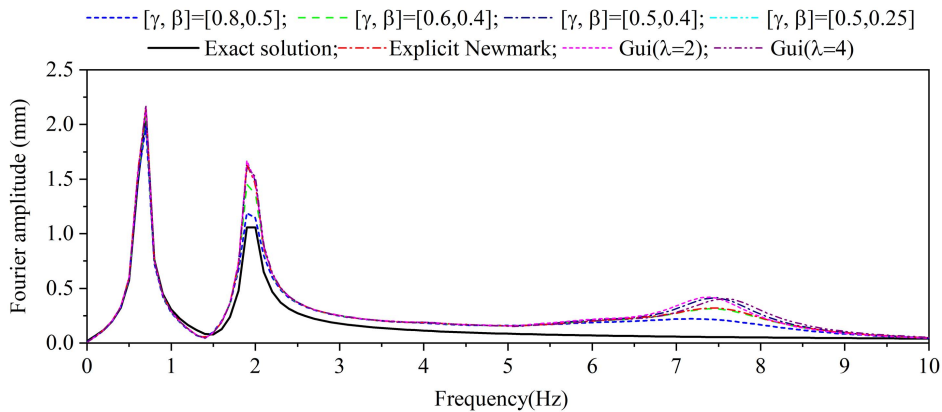


Fig. 13. Frequency-domain displacement response of structure in Case 2.

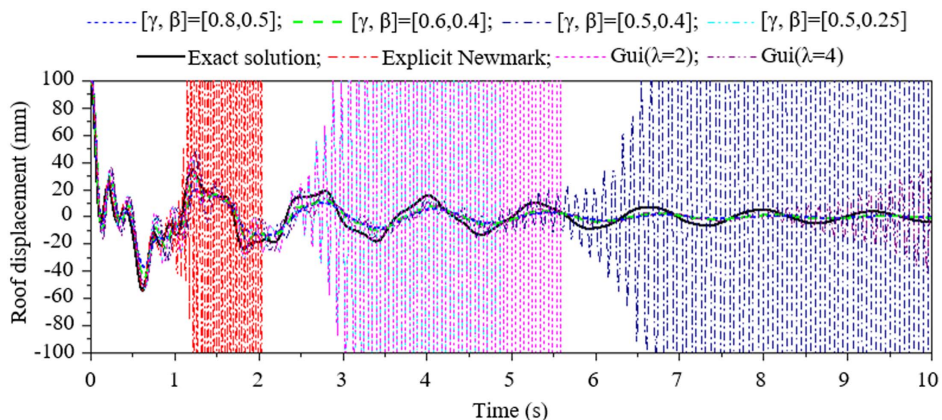


Fig. 14. Time-domain displacement response of structure with time step of 25/1,024 s.

and the former was less accurate than the latter. This is attributed to the numerical damping of SSMEDV algorithms with parameters $[\gamma, \beta] = [0.6, 0.4]$ and $[\gamma, \beta] = [0.8, 0.5]$, which can weaken the high-frequency response caused by a long time step, as shown in Fig. 15.

When the time step continued to increase to 60/1,024 s, Fig. 16 presents that Gui($\lambda = 2$) was unstable, whereas SSMEDV

algorithms with parameters $[\gamma, \beta] = [0.6, 0.4]$ and $[\gamma, \beta] = [0.8, 0.5]$ were still stable, but the accuracy of the algorithms was reduced, so it is not recommended to make the time step too long. Overall, SSMEDV algorithms had better stability than two typical algorithms of the explicit Newmark and Gui- λ .

Finally, because the large scale and complexity of structures lead to an increase in the number of DOFs, the computational

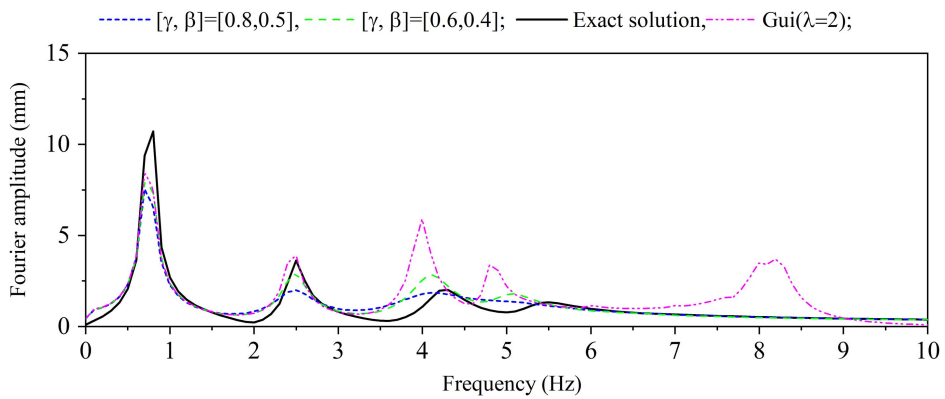


Fig. 15. Frequency-domain displacement response of structure with time step of 25/1,024 s.

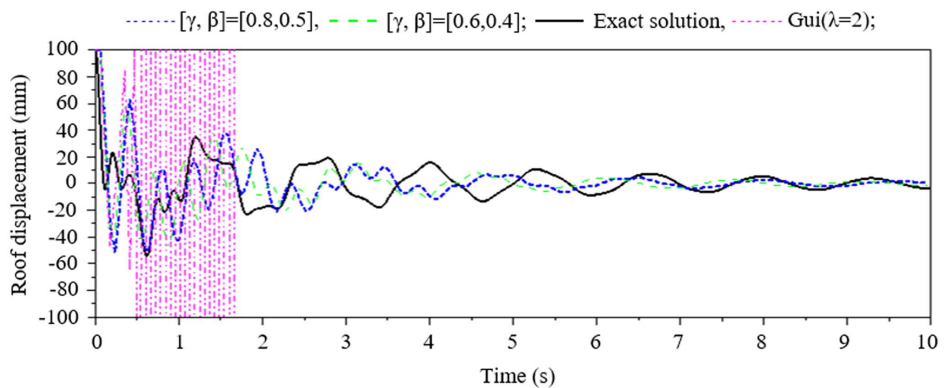


Fig. 16. Time-domain displacement response of structure with time step of 60/1,024 s.

efficiency is particularly important. An example was designed to compare the computational efficiency of algorithms. The model was excited by the combination of 1- and 2-Hz sine waves, which was expressed as follows:

$$F_p = \sum m \times [\sin(4\pi t) + \cos(2\pi t)] \quad (24)$$

The time step is still 10/1,024 s. In Fig. 17, when the number of DOFs was small, all calculation times were basically the same.

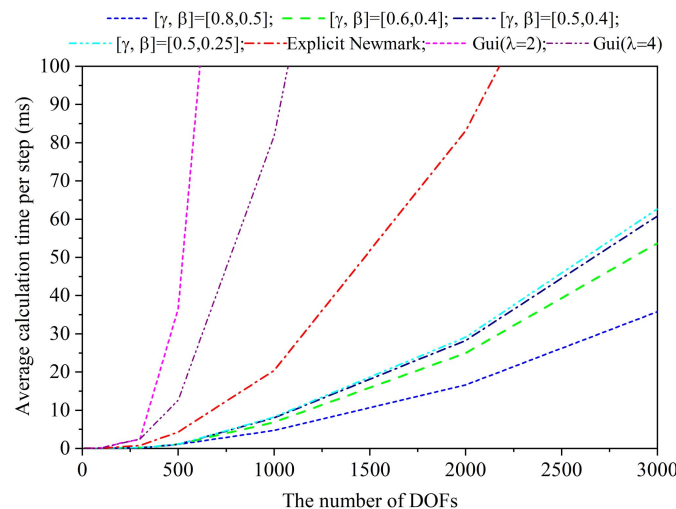


Fig. 17. Calculation time per step under different numbers of DOFs.

When the number of DOFs increased, all calculation times increased significantly, and it is obvious that the computational efficiency of the SSMEDV algorithms was higher than that of other algorithms.

Building–Damper Structure

The SSMEDV algorithms were applied to the RTHS of a building–damper structure under earthquakes. The structure consisted of the numerical substructure of a 9-story frame structure and the physical substructure of a velocity viscous damper, which was a restoring force model based on typical linear damping (Zhou 2006), as shown in Fig. 18.

The structure was excited by the Italian Friuli seismic record in 1976, as shown in Fig. 19, and it indicates that the excellent frequency is 0.64 Hz.

Figs. 20 and 21 show the roof displacement response of the structure obtained by LabVIEW simulation analysis under low-level earthquakes (0.07g) and high-level earthquakes (0.4g), respectively. The result from MATLAB simulation of the whole structure was used as the exact solution, and the time step was 5/1,024 s. The results demonstrate that the algorithms are stable and have good accuracy.

To quantify the error of displacement response curve, the normalized root-mean square error (RMSE) (Luo et al. 2022) was calculated as 3.79% ($\gamma = 0.8$ and $\beta = 0.5$), 3.67% ($\gamma = 0.6$ and $\beta = 0.4$), and 3.68% ($\gamma = 0.5$ and $\beta = 0.4$), which shows that they are similar overall. This is because at this excellent frequency and time step, Ω was 0.02 and the numerical damping of the algorithms was almost the same, as shown in Fig. 6(a). Therefore,

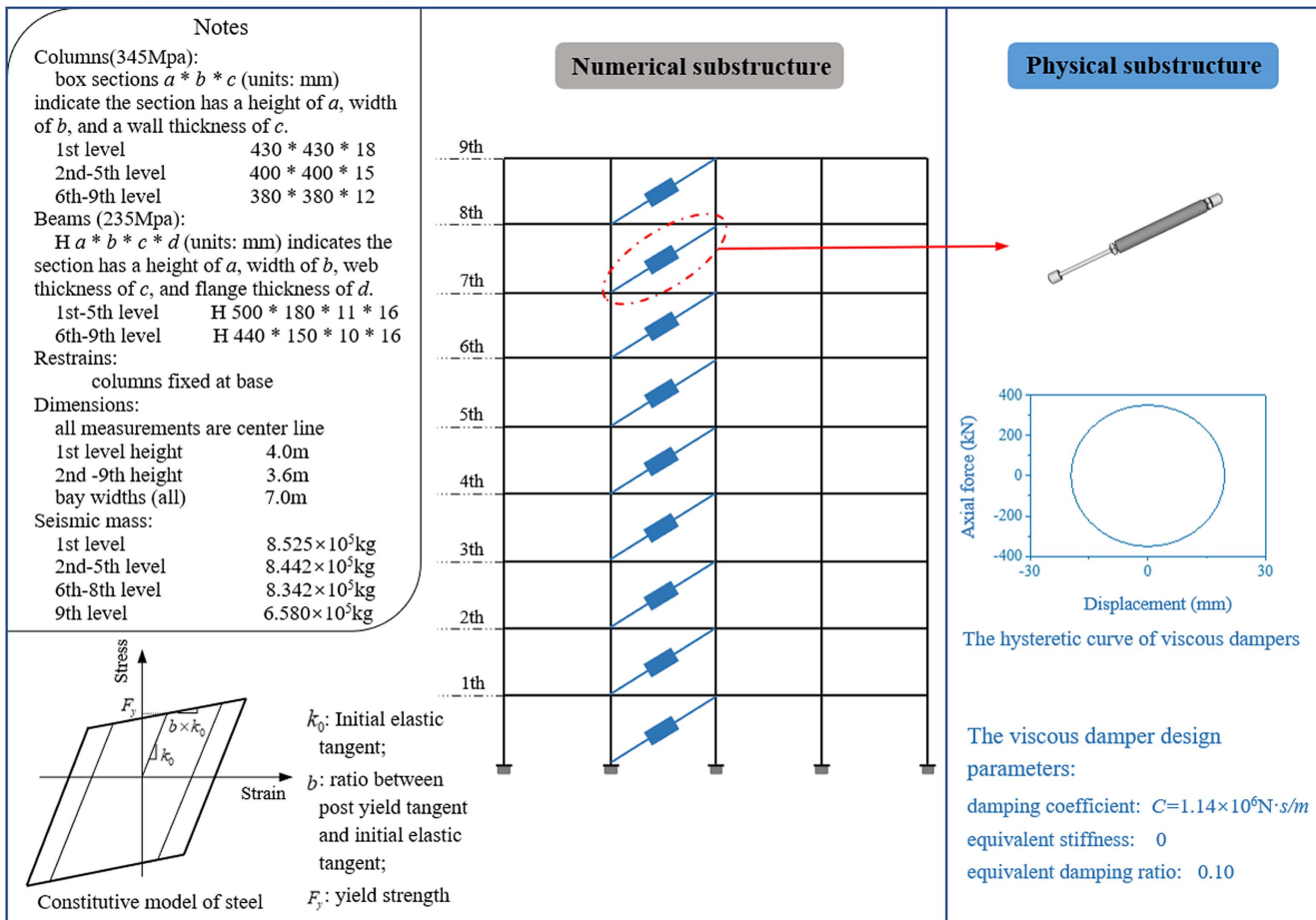


Fig. 18. RTHS of building-damper structure.

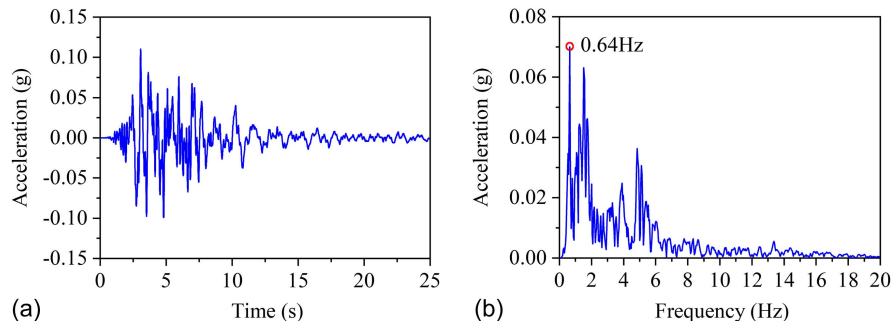


Fig. 19. Acceleration curve of Friuli, Italy, earthquake: (a) time domain; and (b) frequency domain.

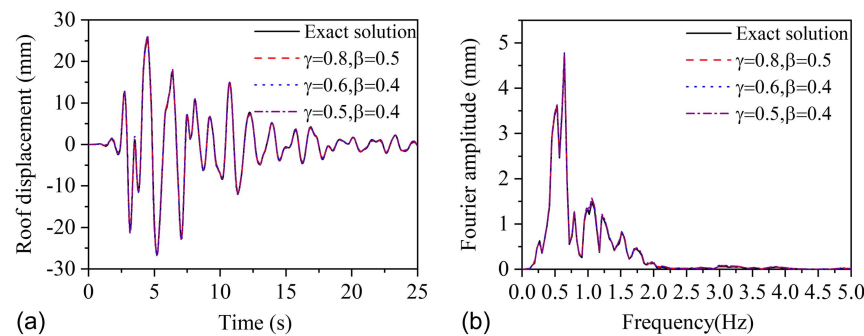


Fig. 20. Displacement response of structure under low-level earthquakes ($0.07g$): (a) time-domain response; and (b) frequency-domain response.

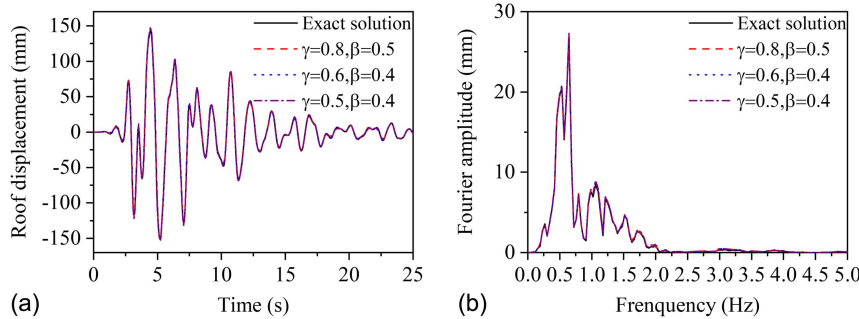


Fig. 21. Displacement response of structure under high-level earthquakes ($0.4g$): (a) time-domain response; and (b) frequency-domain response.

the SSMEDV algorithms can be applied to low-level and high-level earthquakes in RTHS with control error and interpolation algorithms.

Conclusions

The paper presented improved algorithms based on the discrete control theory for conducting RTHS, and they were studied by numerical analysis, MDOF structure, and complex building-damper structure, the following conclusions were drawn:

- The numerical analysis demonstrated that the algorithms have unconditional stability for linear and softening nonlinear structures at $\gamma \geq 0.5$ and $\beta \geq (2\gamma+1)^2/16$, and for a hardening nonlinear structure at the maximum stiffness ratio of 4.04. The algorithms introduce positive numerical damping at $\gamma > 1/2$. The displacement and time step have a one power overshoot effect due to the initial velocity, but the velocity does not.
- Compared with the explicit Newmark algorithm and Gui- λ algorithms, SSMEDV algorithms have adjustable numerical damping to attenuate the high-frequency response. Even though the explicit Newmark algorithm and Gui- λ algorithms are unstable, the proposed algorithms had good stability over long time steps. Moreover, the proposed algorithms had higher computational efficiency than the two typical algorithms. The simulation of building-damper structure indicated that the algorithms can be applied to complex RTHS.
- When $\gamma = 1/2$, SSMEDV algorithms are second-order accurate without any numerical damping, which is suitable for structures with few degrees of freedom or only low-frequency excitation. It is recommended to use $\beta = 0.25$ with a relatively small PE. When $\gamma \neq 1/2$, SSMEDV algorithms are first-order accurate; $\gamma > 1/2$ is necessary to introduce high-frequency dissipation, which is suitable for structures with many degrees of freedom and high-frequency excitation. In addition, $\beta = (2\gamma+1)^2/16$ is recommended for any given value of γ .

Data Availability Statement

All data, models, or code that support the findings of this study are available from the corresponding author upon reasonable request.

Acknowledgments

The authors are grateful for the financial support from the National Natural Science Foundation of China (Project Nos. 51878674 and 52022113) and the Fundamental Scientific Research Expenses of IME, China Earthquake Administration

(Project No. 2020EEEVOL0403). Any opinions, findings, conclusions, or recommendations expressed in this paper are those of the authors.

References

- Chang, S. 2014. "A family of noniterative integration methods with desired numerical dissipation." *Int. J. Numer. Methods Eng.* 100 (1): 62–86. <https://doi.org/10.1002/nme.4720>.
- Chen, C., and J. Ricles. 2008. "Development of direct integration algorithms for structural dynamics using discrete control theory." *J. Eng. Mech.* 134 (8): 676–683. [https://doi.org/10.1061/\(ASCE\)0733-9399\(2008\)134:8\(676\)](https://doi.org/10.1061/(ASCE)0733-9399(2008)134:8(676)).
- Chen, C., and J. Ricles. 2010. "Stability analysis of direct integration algorithms applied to MDOF nonlinear structural dynamics." *J. Eng. Mech.* 136 (4): 485–495. [https://doi.org/10.1061/\(ASCE\)EM.1943-7889.0000083](https://doi.org/10.1061/(ASCE)EM.1943-7889.0000083).
- Chen, C., J. Ricles, T. Marullo, and O. Mercan. 2009. "Real-time hybrid testing using the unconditionally stable explicit CR integration algorithm." *Earthquake Eng. Struct. Dyn.* 38 (1): 23–44. <https://doi.org/10.1002/eqe.838>.
- Chopra, A. 2001. *Dynamics of structures: Theory and applications to earthquake engineering*. 2nd ed. Upper Saddle River, NJ: Prentice Hall.
- Enokida, R., D. Stoten, and K. Kajiwara. 2015. "Stability analysis and comparative experimentation for two substructuring schemes, with a pure time delay in the actuation system." *J. Sound Vib.* 346 (23): 1–16. <https://doi.org/10.1016/j.jsv.2015.02.024>.
- Feng, Y., Z. X. Guo, and Y. C. Gao. 2018. "An unconditionally stable explicit algorithm for nonlinear structural dynamics." *J. Eng. Mech.* 144 (6): 04018034. [https://doi.org/10.1061/\(ASCE\)EM.1943-7889.0001458](https://doi.org/10.1061/(ASCE)EM.1943-7889.0001458).
- Franklin, G. F., J. D. Powell, and N. Emami. 2002. *Feedback control of dynamic systems*. Upper Saddle River, NJ: Prentice Hall.
- Fu, B., D. C. Feng, and H. Jiang. 2019. "A new family of explicit model-based integration algorithms for structural dynamic analysis." *Int. J. Struct. Stab. Dyn.* 19 (6): 1950053. <https://doi.org/10.1142/S0219455419500536>.
- Goudreau, G. L., and R. L. Taylor. 1973. "Evaluation of numerical integration methods in elastodynamics." *Comput. Methods Appl. Mech. Eng.* 2 (1): 69–97. [https://doi.org/10.1016/0045-7825\(73\)90023-6](https://doi.org/10.1016/0045-7825(73)90023-6).
- Gu, Q., D. Zhang, W. Guo, J. Wu, B. Yuan, H. Zhou, and T. Wang. 2021. "An efficient computation method for real-time hybrid testing of vehicle-track-bridge coupling system of high-speed railway." *J. South China Univ. Technol.: Nat. Sci. Ed.* 49 (3): 123–130. <https://doi.org/10.12141/j.issn.1000-565X.200322>.
- Gui, Y., J. Wang, F. Jin, C. Chen, and M. Zhou. 2014. "Development of a family of explicit algorithms for structural dynamics with unconditional stability." *Nonlinear Dyn.* 77 (4): 1157–1170. <https://doi.org/10.1007/s11071-014-1368-3>.
- Guo, J., Z. Tang, S. Chen, and Z. Li. 2016. "Control strategy for the substructuring testing systems to simulate soil-structure interaction." *Smart Struct. Syst.* 18 (6): 1169–1188. <https://doi.org/10.12989/sss.2016.18.6.1169>.

- Guo, W., Z. Zhai, H. Wang, Q. Liu, K. Xu, and Z. Yu. 2019. "Shaking table test and numerical analysis of an asymmetrical twin-tower super high-rise building connected with long-span steel truss." *Struct. Des. Tall Spec.* 28 (13): e1630. <https://doi.org/10.1002/tal.1630>.
- Huang, L., C. Chen, M. Chen, and T. Guo. 2022. "Effect of time-varying delay on stability of real-time hybrid simulation with multiple experimental substructures." *J. Earthquake Eng.* 26 (1): 357–382. <https://doi.org/10.1080/13632469.2019.1688735>.
- Jiang, H., Y. Ying, B. Wang, and Y. Zhang. 2012. "Experiment on seismic damage behavior of RC shear walls." *Build. Struct.* 42 (2): 113–117. <https://doi.org/10.19701/j.jzjg.2012.02.023>.
- Kolay, C., and J. Ricles. 2014. "Development of a family of unconditionally stable explicit direct integration algorithms with controllable numerical energy dissipation." *Earthquake Eng. Struct. Dyn.* 43 (9): 1361–1380. <https://doi.org/10.1002/eqe.2401>.
- Kolay, C., and J. Ricles. 2019. "Improved explicit integration algorithms for structural dynamic analysis with unconditional stability and controllable numerical dissipation." *J. Earthquake Eng.* 23 (5): 771–792. <https://doi.org/10.1080/13632469.2017.1326423>.
- Li, N., X. Lu, Z. Zhou, and Z. Li. 2021. "Study on the stability of real-time substructure test considering numerical integration algorithm." *Eng. Mech.* 38 (11): 12–22. <https://doi.org/10.6052/j.issn.1000-4750.2020.10.0767>.
- Li, X., A. Ozdagli, S. Dyke, X. Lu, and R. Christenson. 2017. "Development and verification of distributed real-time hybrid simulation methods." *J. Comput. Civ. Eng.* 31 (4): 1–14. [https://doi.org/10.1061/\(ASCE\)CP.1943-5487.0000654](https://doi.org/10.1061/(ASCE)CP.1943-5487.0000654).
- Liang, X., and K. M. Mosalam. 2016. "Lyapunov stability analysis of explicit direct integration algorithms considering strictly positive real lemma." *J. Eng. Mech.* 142 (10): 04016079. [https://doi.org/10.1061/\(ASCE\)EM.1943-7889.0001143](https://doi.org/10.1061/(ASCE)EM.1943-7889.0001143).
- Luo, Y., W. Fu, H. Wan, and Y. Shen. 2022. "Load-effect separation of a large-span prestressed structure based on an enhanced EEMD-ICA methodology." *J. Struct. Eng.* 148 (3): 1–15. [https://doi.org/10.1061/\(ASCE\)ST.1943-541X.0003263](https://doi.org/10.1061/(ASCE)ST.1943-541X.0003263).
- Nakashima, M., H. Kato, and E. Takaoka. 1992. "Development of real-time pseudo dynamic testing." *Earthquake Eng. Struct. Dyn.* 21 (1): 79–92. <https://doi.org/10.1002/eqe.4290210106>.
- Newmark, N. 1959. "A method of computation for structural dynamics." *J. Eng. Mech.* 85 (3): 67–94. <https://doi.org/10.1061/JMCEA3.0000098>.
- Peng, P. 2016. *Development of online hybrid testing: Theory and applications to structural engineering*. Beijing: Tsinghua University Press.
- Rezaiee-Pajand, M., S. Esfehani, and H. Ehsanmanesh. 2021. "An efficient weighted residual time integration family." *Int. J. Struct. Stab. Dyn.* 21 (8): 2150106. <https://doi.org/10.1142/S0219455421501066>.
- Tang, Y., D. Ren, H. Qin, and C. Luo. 2021. "New family of explicit structure-dependent integration algorithms with controllable numerical dispersion." *J. Eng. Mech.* 147 (3): 1–18. [https://doi.org/10.1061/\(ASCE\)EM.1943-7889.0001901](https://doi.org/10.1061/(ASCE)EM.1943-7889.0001901).
- Wang, J., and H. Zhang. 2017. "Seismic performance assessment of blind bolted steel-concrete composite joints based on pseudo-dynamic testing." *Eng. Struct.* 131 (11): 192–206. <https://doi.org/10.1016/j.engstruct.2016.11.011>.
- Wu, B., H. Bao, J. Ou, and S. Tian. 2005. "Stability and accuracy analysis of the central difference method for real-time substructure testing." *Earthquake Eng. Struct. Dyn.* 34 (7): 705–718. <https://doi.org/10.1002/eqe.451>.
- Wu, B., L. Deng, and X. Yang. 2009. "Stability of central difference method for dynamic real-time substructure testing." *Earthquake Eng. Struct. Dyn.* 38 (27): 1649–1663. <https://doi.org/10.1002/eqe.927>.
- Wu, B., G. Xu, Q. Wang, and M. S. Williams. 2006. "Operator-splitting method for real-time substructure testing." *Earthquake Eng. Struct. Dyn.* 35 (3): 293–314. <https://doi.org/10.1002/eqe.519>.
- Yang, C., X. Wang, Q. Li, and S. Xiao. 2020. "An improved explicit integration algorithm with controllable numerical dissipation for structural dynamics." *Arch. Appl. Mech.* 90 (11): 2413–2431. <https://doi.org/10.1007/s00419-020-01729-9>.
- Yang, C., B. Yang, T. Zhu, and S. Xiao. 2017. "Comparison and assessment of time integration algorithms for nonlinear vibration systems." *J. Cent. South Univ.* 24 (5): 1090–1097. <https://doi.org/10.1007/s11771-017-3512-y>.
- Yu, J., X. Meng, B. Yan, B. Xu, Q. Fan, and Y. Xie. 2019. "Global navigation satellite system-based positioning technology for structural health monitoring: A review." *Struct. Control Health Monit.* 27 (1): 1545–2255. <https://doi.org/10.1002/stc.2467>.
- Zhou, Y. 2006. *Design of structures with viscous dampers*. Wuhan, China: Wuhan University of Technology Press.
- Zhu, F., J. Wang, F. Jin, F. Chi, and Y. Gui. 2015. "Stability analysis of MDOF real-time dynamic hybrid testing systems using the discrete-time root locus technique." *Earthquake Eng. Struct. Dyn.* 44 (2): 221–241. <https://doi.org/10.1002/eqe.2467>.
- Zhu, F., J. Wang, F. Jin, and Y. Gui. 2016. "Comparison of explicit integration algorithms for real-time hybrid simulation." *Bull. Earthquake Eng.* 14 (1): 89–114. <https://doi.org/10.1007/s10518-015-9816-0>.
- Zhu, F., J. Wang, F. Jin, and L. Lu. 2019. "Control performance comparison between tuned liquid damper and tuned liquid column damper using real-time hybrid simulation." *Earthquake Eng. Eng. Vib.* 18 (3): 695–701. <https://doi.org/10.1007/s11803-019-0530-9>.